targeted to clathrin (C, D) and early endosomes (E, F). Interestingly, exogenously added rhCCN2 and, particularly, the recycling endosome marker were predominantly co-localized in HCS-2/8 cells (I, J). Merge: merged images of rhCCN2 with LRP1 (C, D), clathrin (E, F), EEA1 (G, H), or Rab11 (I, J) staining. Scale bars, 5 μm.

Fig. 3. Effect of LRPAP1 on CCN2 transcytosis in chondrocytes. (A) Schemaic representation of the sampling strategy is shown. E. coli-derived dual-tagged CCN2 (B, C) was added to control or LRPAP1-treated HCS-2/8 cells in the upper chamber of a Transwell, the medium in the upper chamber was removed after 1 h; and the cellular protein (**B**) and the medium in the lower chamber (**C**) were collected as illustrated. Immunoblotting was performed by using anti-Flag or His tag antibody. As a result, the bound/ incorporated (**B**) and transcytosed (**C**) amount of CCN2 was decreased in the LRPAP1-treated HCS-2/8 cells. Comparable results were obtained with HeLa cell-derived biotinylated recombinant CCN2 detected by the Streptavidin conjugate (D, E). Positions of molecular weight markers (35, 75 kDa) are shown at the right of the images. NC, the mixture of anti-FLAG® M2 affinity gel or Ni-NTA−agarose gel and serum-free D-MEM without Flag or His-fusion protein as a negative control.

Fig. 4. Effect of hypoxia on levels of LRP1 mRNA and protein in HCS-2/8 cells. (**A**) The *LRP1* mRNA level in HCS-2/8 cells under hypoxia. The level of mRNA was standardized to that of *18s* mRNA. Exposure to hypoxia resulted in a time-dependent increase in the *LRP1* mRNA level. The values represent the means ± SD. $^*P < 0.05$. (**B**) LRP1, CCN2 and HIF1α protein level in HCS-2/8 cells under hypoxia for 48 h. Immunoblotting was carried out with anti-LRP1, CCN2 and HIF1α antibody. Stronger signals for the LRP1 subunit, CCN2 and HIF1α were detected under hypoxia. (**C**) Effect of antisense HIF1α oligonucleotides on HIF1α, LRP1 and CCN2 production under hypoxic condition for 48 h. Treating the cells in 5% O_2 with antisense

oligonucleotides to HIF1α (AS-HIF) for 48 h abolished LRP1, CCN2 and HIF1α production. S-HIF: control experiments with the sense oligonucleotide. The position of the molecular weight marker used (35 and 75 kDa) is shown at the left of the images.

Fig. 5. Effect of hypoxia on CCN2 transcytosis in chondrocytes. Transcytosis assay was performed as described in the legend of Figure 2. As a result, the bound/ incorporated (**A**) and transcytosed (**B**) amount of CCN2 increased in the HCS-2/8 cells under hypoxia, and the increase was suppressed by LRPAP1. NC, the mixture anti-FLAG® M2 affinity gel or Ni-NTA−agarose gel and serum free D-MEM without Flag or His-fusion protein as a negative control.

Fig. 6. LRPAP1 in HeLa, MDA-231, and HCS-2/8 cells. (**A**) The mRNA level of *LRP1* and *LRPAP1* in HeLa, MDA-231, and HCS-2/8 cells. The level of each mRNA was standardized to that of *GAPDH* mRNA. *LRP1* and *LRPAP1* mRNAs were highly expressed in chondrocytic HCS-2/8 cells. The values represent the means ± SD. $*P < 0.05$. (**B**) The protein level of LRPAP1 in HeLa, MDA-231, and HCS-2/8 cells. Immunoblotting was carried out with anti-LRPAP1 antibody. The strongest signal for the LRPAP1 was detected in the HCS-2/8 cells. Positions of molecular weight markers (35kDa) are shown at the right of the images.

Fig. 7. Difference in expression and distribution of LRPAP1 among chondrocytes of various differentiation stages. (**A**) Immunohistochemical analysis of LRPAP1 in the growth plate. Tibial sections from mice were stained with anti-LRPAP1 antibody. The ECM in the entire growth-plate cartilage was immunopositive for LRPAP1, with the strongest signal in the resting zone. The dark gray circles in the bottom panel represent the cells that express *Ccn2* gene. The hatched circles therein represent the cells that accumulated CCN2 protein. Scale bars, 2 mm. (**B**) Change in the

expression levels of *lrpap1* mRNA and other mRNAs in chicken sternum chondrocytes of various differentiation stages. LC, USP, and USC represent resting, proliferating, and hypertrophic chondrocytes in the growth plate, respectively. The expression of *lrpap1* mRNA was the highest in the LC cells. Thus these results support the data obtained in vivo (**A**). The values represent the means ± SD. $*P < 0.05$.

Fig. 8. Schematic representation of the molecular mechanism determining the polarity of CCN2 distribution. CCN2 protein is transported from prehypertrophic chondrocytes, where it is produced, through transcytosis mediated by LRP1 to the hypertrophic chondrocytes. The high levels of LRPAP1 in the resting zone interfere with this transportation, whereas this interference is presumably attenuated by down-regulation of LRPAP1 in the hypertrophic layer and down-regulation of LRP1 by oxygen in the late hypertrophic layer. As a result of the down-regulation of LRP1 by oxygen in the late hypertrophic layer, CCN2 is accumulated in the hypertrophic layer.

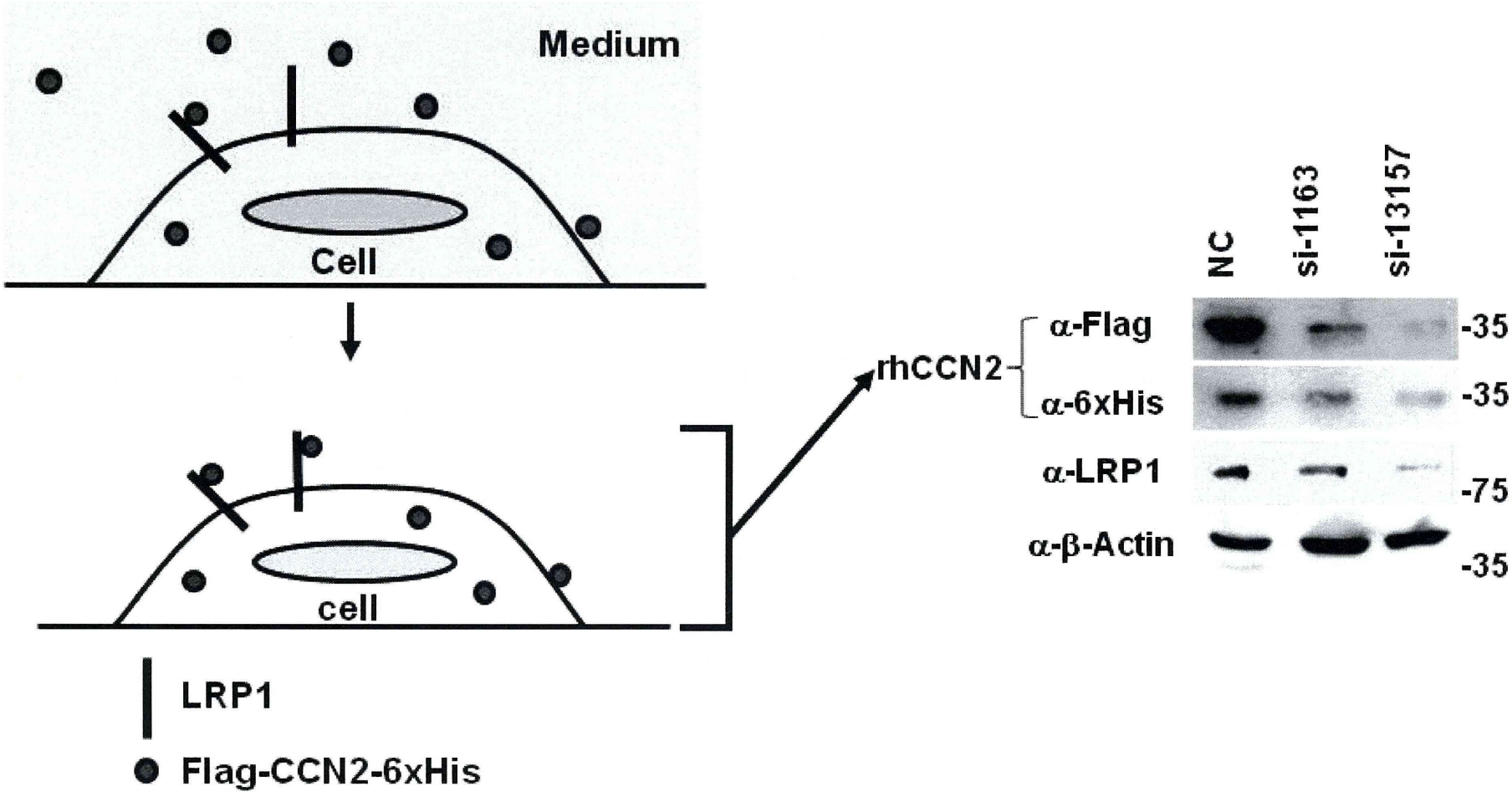

Fig. 1

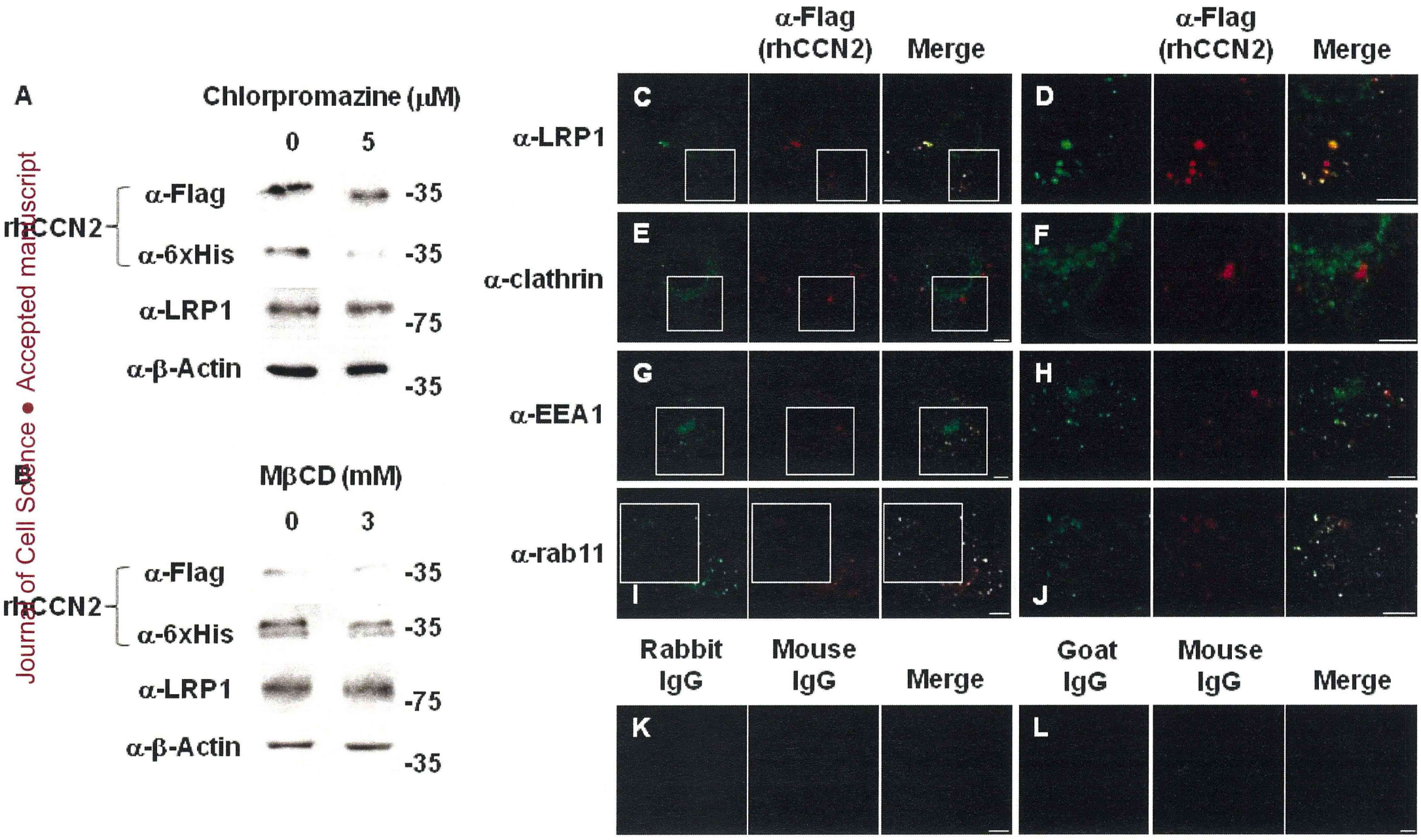

Fig. 2

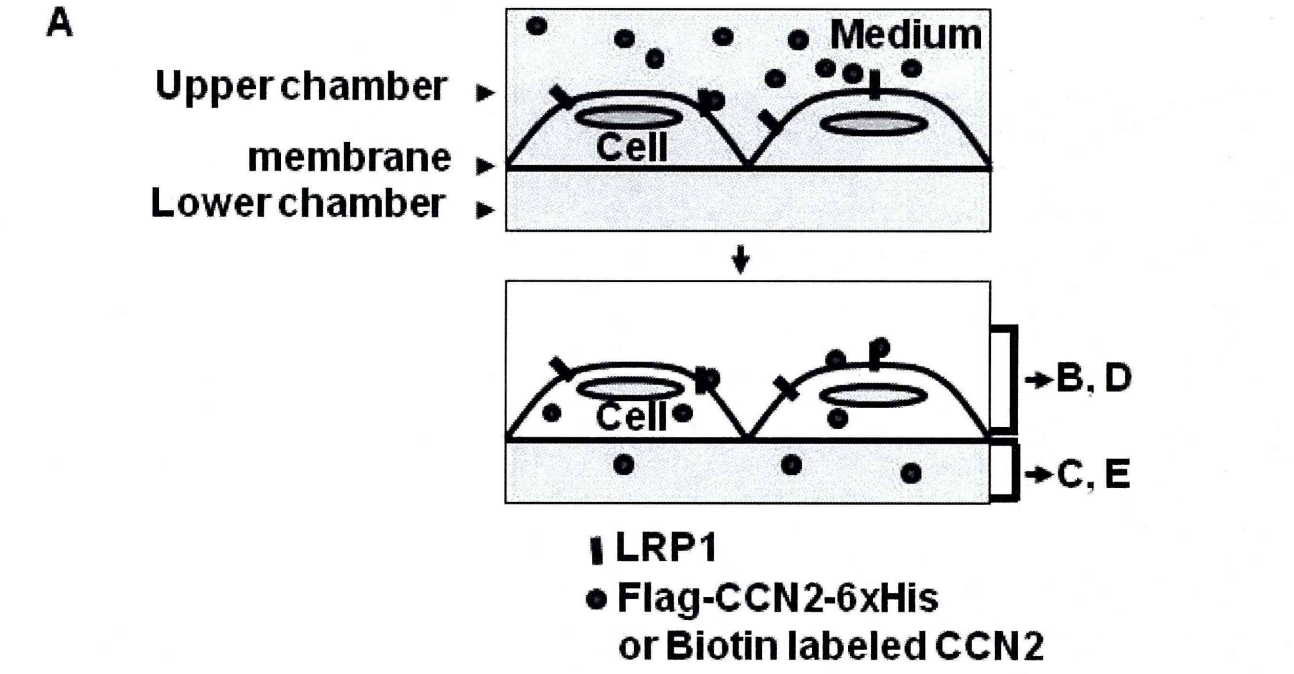

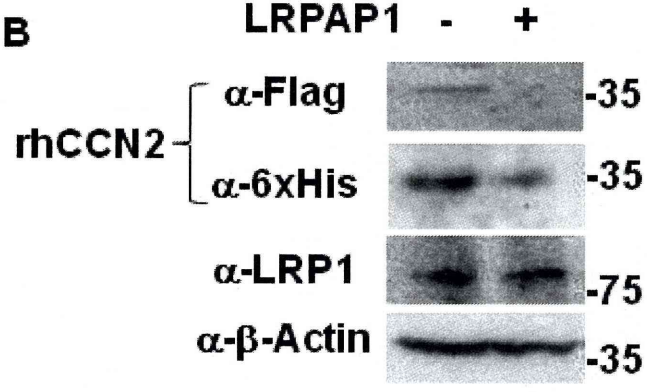

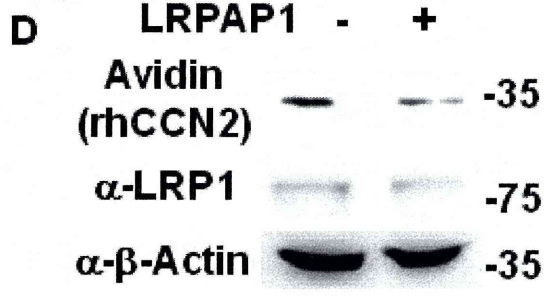

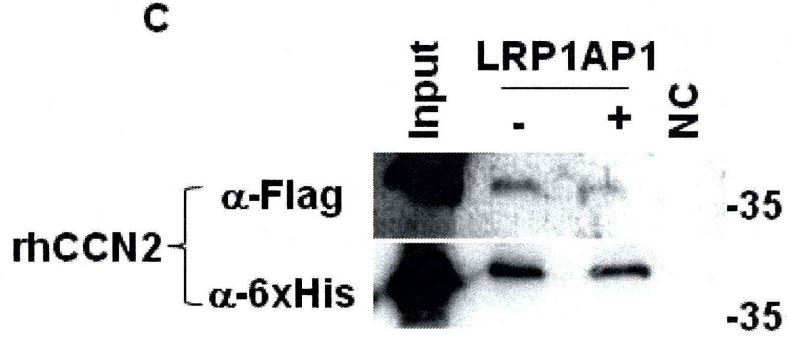

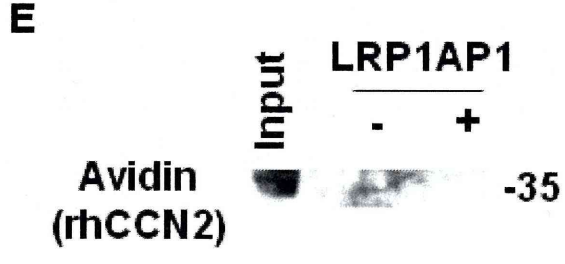

Fig. 3

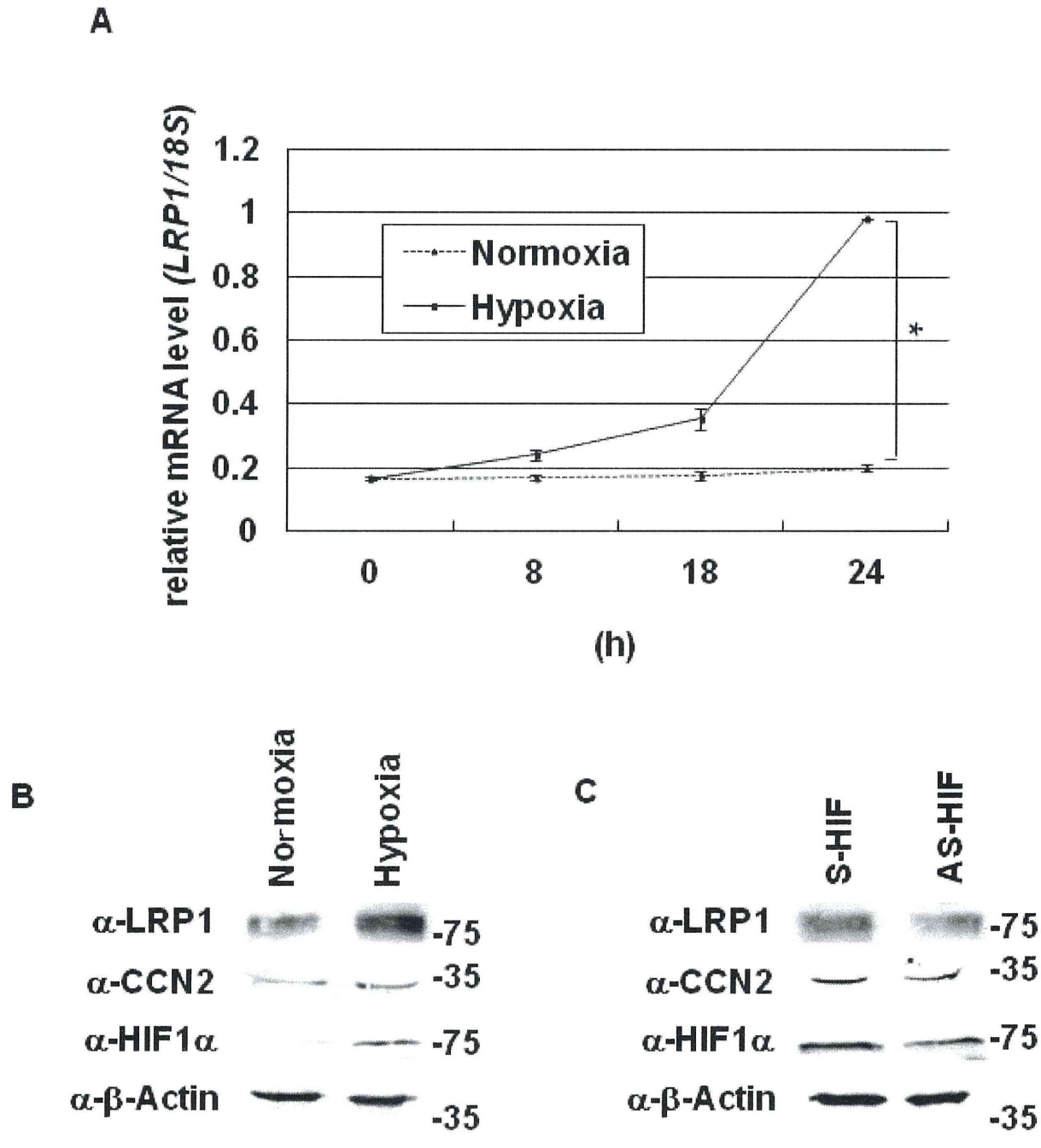

Fig. 4

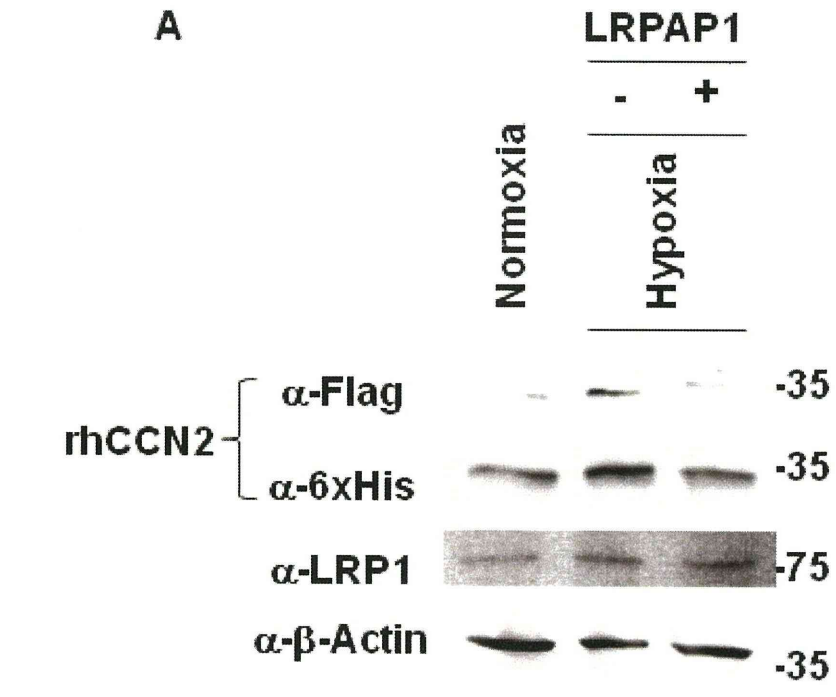

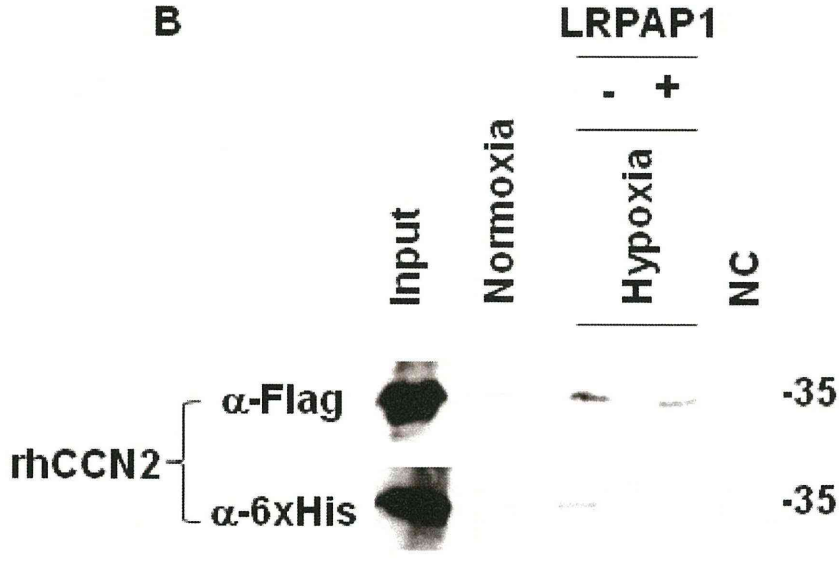

Fig. 5

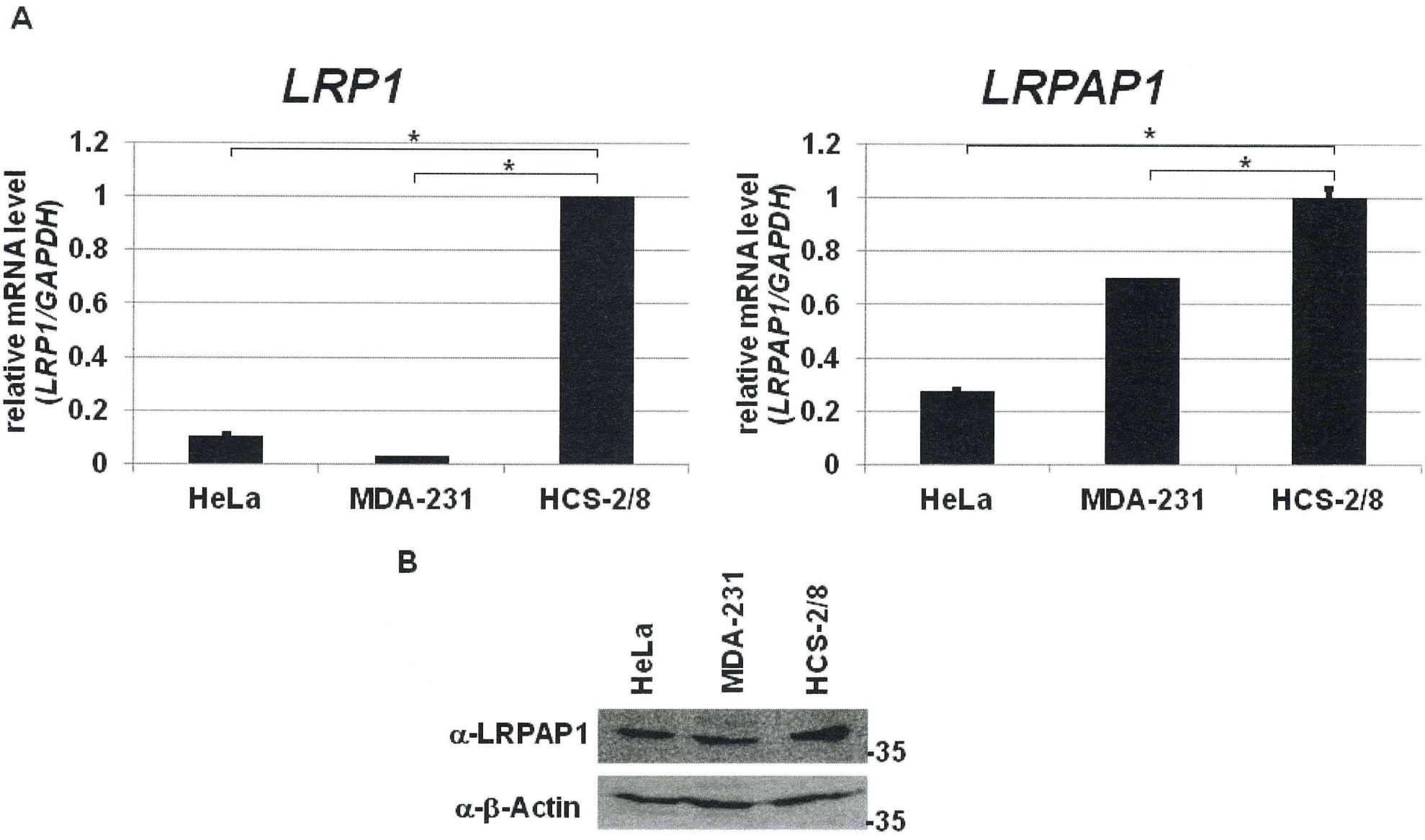

Fig. 6

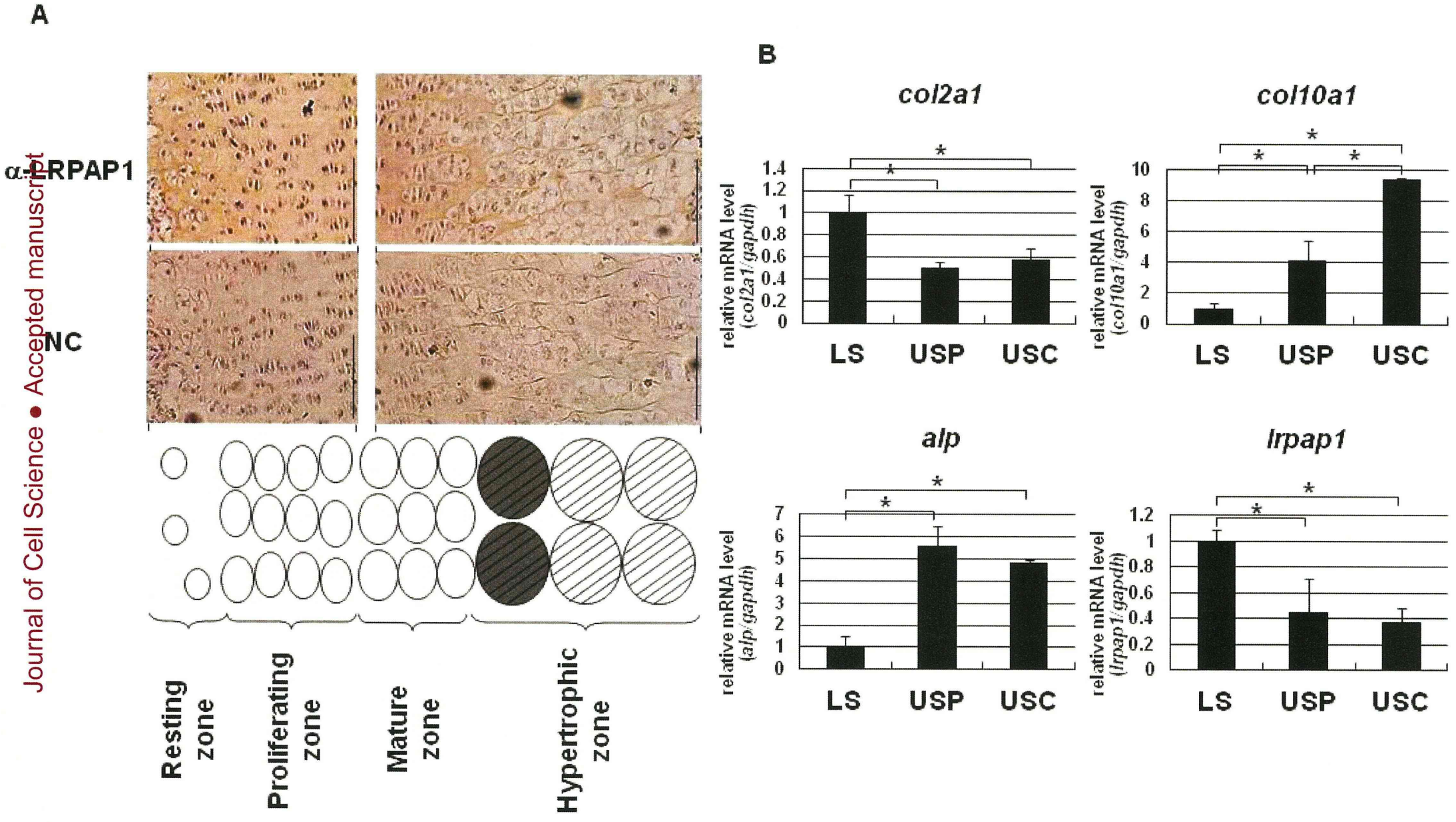

Fig. 7

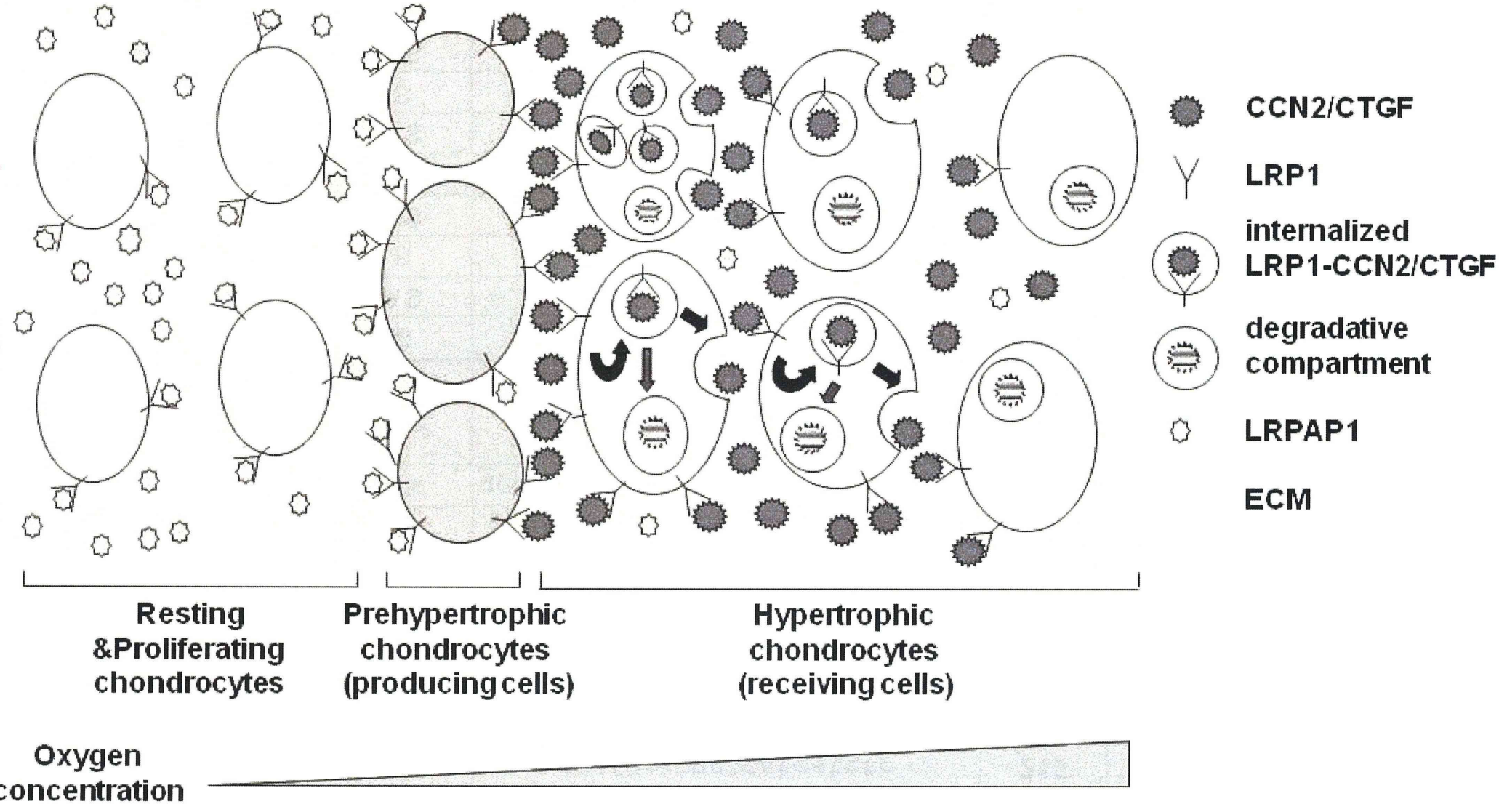

Fig. 8

Table 1.

Primers and experimental conditions for real-time PCR

target gene (human)	Primer direction	Sequence(5'→3')	Length of PCR product	Annealing temperature (℃)
GAPDH	S	gccaaaagggtcatcatctc	215	65
	AS	gtcttctgggtggcagtgat		
LRP1	S	acatatagcctccatcctaatc	152	65
	AS	ttccaatctccacgttcat		
LRPAP1	S	ctgaggctgagttcgaggag	150	65
	AS	gctgcttctggtagtggttg		
18S	S	gcgaattcctgccagtagcatatgcttg	140	60
	AS	ggaagcttagaggagcgagcgaccaaagg		
Target gene (chicken)				
gapdh	S	aggctgtggggaaagtca	202	65
	AS	gacaacctggtcctctgtgtat		
col2a1	S	agaaaggaatccagcccaat	236	65
	AS	acacctgccagattgattcc		
col10a1	S	acatgcatttacaaatatcgttac	160	60
	AS	aaaatagtagacgttaccttgactc		
alp	S	aacggccctggctataagat	186	60
	AS	tgggggatgtagttctgctc		
lrpap1	S	acccggtgaaagaggaagtc	164	65
	AS	tgccatgtcccacaaatc		

S, sense; AS, anti-sense.

Classical Models of Senile Osteoporosis

10

Ken Watanabe

10.1 Introduction

Most vertebrates exhibit age-related decline in physiological function, particularly in locomotion. Loss of muscle volume and bone mass in late life is a hallmark of aging and resembles tissue obsolescence caused by disuse. However, some human populations lose bone mass more rapidly than would be predicted by normal aging. These individuals are diagnosed as having senile osteoporosis, one of the most prevalent geriatric disorders and one that seriously decreases quality of life in the elderly. As noted throughout this book, mice and rats are the most frequently used models to study osteoporosis, its treatment and prevention, and concomitant pathogenesis. Both mice and rats have an approximately 3-year lifespan. Bone mass peaks within the first quarter of life and then declines with age. This chapter describes age-related bone loss in laboratory rodents.

10.2 Aged Mice

Significant decreases in bone mass during the latter half of life are observed in laboratory rodents, such as mice and rats. Most studies of aged rodents focus on the anatomy and mechanism of age-related bone loss, a critical factor for senile osteoporosis, but the phenomenon can also be seen as part of the normal aging process. In most studies of senescence, mice of 18–30 months of age are used as models of aging. However, genetic manipulation of mice to study aging may require 2 years before a particular phenotype emerges, making it difficult for a postdoc to complete the study or to attain grant support. Fortunately, although the sources and strains are still limited, aged mice can be obtained from some resources, such as the National Institute on Aging (NIA, USA), which provides aged rodents only for academic and nonprofit research institutes.

Among mouse strains, C57BL/6 is most often used to study age-related bone loss. Age-related changes in bone structure and skeletal mass seen in this strain are reportedly representative of those observed in human aging.[1-4] One study showed that bone volume/tissue volume (BV/TV), trabecular number (Tb.N), and connectivity decrease with age, whereas cortical thickness increases between 6 weeks and 6 months of age and then declines.[3] In the same study, cortical area (Ct.Ar) was not markedly changed between 6 and 24 months, and skeletal tissue weight of the tibia defatted by organic solvents was maximal at 12 months of age and then the fat-free weight decreased. The male mice used in this study showed no changes in serum testosterone level, suggesting that age-related bone loss in male C57BL/6 mice is apparently independent of androgen deficiency.[3] Female mice do not appear to experience menopause but show age-related retardation of estrous cycles.[5] Age-related bone loss in trabecular bones of vertebra and femora is more pronounced in female *mice*,[2] which show decreases in trabecular bone as early as 2–6 months of age. However, age-related changes in the parameters of bone formation and resorption differ among femoral mid-diaphysis, metaphysis, and lumbar vertebrae, which also differ in composition of trabecular and cortical bones and in mechanical properties.[1,2,4] Serum markers of aged C57BL/6 mice suggest a high

K. Watanabe
Department of Bone and Joint Disease, National Center for Geriatrics and Gerontology, Obu, Aichi, Japan
e-mail: kwatanab@ncgg.go.jp

G. Duque and K. Watanabe (eds.), *Osteoporosis Research*,
DOI: 10.1007/978-0-85729-293-3_10,

turnover state of bone metabolism after 24 months of age.[4] Assessment of mechanical properties by three-point flexure tests also reveals that the long bones are maturing between 3 and 10 months of age.[1] From time points representing peak bone mass, parameters such as bone mass, whole bone stiffness, and energy to fracture decrease by 24 months of age, whereas periosteal perimeter and cross-sectional moments of inertia continue to increase until 24 months. The growing phase when bone formation predominates ends and the lacuno-canalicular network of osteocytes is well aligned by 3 months of age, corresponding to the time of mechanical maturity.[6]

Among factors regulating osteoclastogenesis, receptor activator of NF-κB ligand (RANKL) expression increases with age, but expression of osteoprotegerin (OPG), a decoy RANK inhibitor, slightly decreases. In mice, RANKL expression is inversely correlated with trabecular bone volume in terms of age-related changes.[7] Such age-related expression patterns are reproduced in *ex vivo* culture of the bone marrow adherent cell fraction within 7 days but diminish in longer-term cultures [Add] (~28 days). Expression of M-CSF, another factor critical for osteoclastogenesis, also increases in the bone marrow of aged mice.[8] When osteoclast differentiation is induced by only RANKL and M-CSF without stromal cells, a greater number of osteoclasts are generated from bone marrow of aged mice compared to younger mice, suggesting that the osteoclast precursor pool increases with age.[8] Thus, both stromal and hematopoietic factors associated with osteoclastogenesis are elevated upon aging, suggesting a correlation with age-related bone loss.

Insulin-like growth factor (IGF) is a well-known factor governing cell survival and somatic tissue growth and maintenance. IGF acts as an anabolic agent for bones as well as muscles and cartilage.[9,10] In aged C57BL/6 mice, growth stimulatory and survival activities of IGF significantly decrease.[11] Although expression of the IGF-1 receptor in aged mice is increased, receptor responsiveness, as evidenced by downstream MAPK and PI3K activation, is markedly reduced. Intermittent treatment with parathyroid hormone (PTH) is known to be a potential anabolic therapy among few other candidates.[12] Knopp et al. reported that 18-month-old C57BL/6 mice exhibit more pronounced increases in spinal bone mineral density (BMD) than do their 3-month-old counterparts in response to intermittent PTH injections, but those increases are not seen in the femur.[13] Mechanical stress plays critical roles in development and maintenance of the skeletal system, including bones. Low-magnitude cyclic loading, which stimulates bone formation in young mice, is not sufficient to initiate bone formation in 21-month-old mice.[14] Thus, either responsiveness to various anabolic stimuli is impaired or the response threshold is shifted, or both occur in the aged skeleton.

10.3 Senescence-Accelerated Mice

The senescence-accelerated mouse (SAM), developed by Takeda's Lab at Kyoto University, originated from the AKR/J strain.[15] SAM strains fall into two categories: P (senescence-prone) inbred strains, which exhibit an accelerated aging phenotype, and R (senescence-resistant) strains, which age normally. Several SAM strains are now commercially available. Among them, SAMP6 is often used as a mouse model of senile osteoporosis.[16] SAMP6 mice show frequent fractures in their tibias and exhibit low peak bone mass, which underlies the accelerated age-related osteoporotic phenotype. Jilka et al. determined the cellular basis of the SAMP6 phenotype and found that the number of osteoblast progenitors in the bone marrow was not altered in this strain at prepuberty (1 month) but decreased significantly at adult ages (~4 months).[17] Age-dependent decreases in BMD were also observed. A decline of histomorphometrical analysis parameters was pronounced not only in bone formation but also in resorption, resulting in reduced bone turnover. The number of osteoclasts in vertebra and femur was significantly reduced, and osteoclast formation in *ex vivo* bone marrow culture was markedly decreased. When bone marrow cells were cocultured with osteoblasts from wild-type mice, osteoclast formation from SAMP6 bone marrow cells was even higher than that seen in the control strain, suggesting that defects in osteoclast formation are caused by impairment in supporting roles of the osteoblast/stromal cell fraction. The authors of this study concluded that the decreased bone mass phenotype seen in SAMP6 mice was due to defects in osteoblastogenesis.[17] Such defects in SAMP6 mice also promote resistance to bone loss following sex hormone deficiency induced by gonadectomy.[18] Increased adipogenesis in the bone marrow of the SAMP6 strain has also been observed, and

expression of an anti-adipogenic cytokine, interleukin-11, was decreased in bone marrow stromal cells of this strain.[19,20] Silva et al. reported that bone-forming activity of SAMP6 osteoblasts is normal, although the number of osteoblasts in the bone marrow was markedly reduced.[21-23] From 2 to 12 months of age, calcein-labeled surfaces in SAMP6 femur and tibia were significantly decreased in endocortical surfaces (inside the long bones) but not in periosteal surfaces (outside the bone), suggesting that SAMP6 mice possess a marrow defect.[23] Interestingly, bone marrow transplantation from normal to recipient SAMP6 mice resulted in a significant increase in trabecular bone and BMD.[24-26] This finding confirms that the defect in SAMP6 mice originates in bone marrow and can be rescued by normal marrow.

The SAMP6 strain has been used to conduct a whole genome scan for quantitative trait loci (QTLs) to identify determinants of bone mass.[27-29] Shimizu et al. analyzed QTLs of the F2 progeny obtained by crossing SAMP6 and SAMP2 mice, the latter of which possesses higher peak bone mass at 4 months of age.[29] In their study they determined cortical thickness of femurs and identified three *peak bone density* (*Pbd*) loci on chromosomes 11, 13, and X, corresponding to *Pbd1*, *Pbd2*, and *Pbd3*, respectively. They developed a congenic strain P6.P2-Pbd2, which possesses the genomic region from SAMP2 chromosome 13 that carries *Pbd2*, on a SAMP6 background. The congenic strain exhibited significantly higher peak bone mass than did SAMP6 mice.[28] Among the genes on the chromosome 13 locus, secreted frizzled-related protein 4 (Sfrp4) expression was significantly elevated in SAMP6 calvaria.[27] Sfrp4 is an antagonist of Wnt ligands and thus inhibits Wnt-β-catenin signaling, which plays an important role in regulating bone mass. Recombinant SFRP4 protein suppressed osteoblast proliferation *in vitro*, suggesting that elevated *Sfrp4* expression underlies decreased bone formation seen in SAMP6 mice.[27]

10.4 Rat Models of Aging

The aging rat also represents a good model to study age-related bone loss.[30-35] Like C57BL/6 mice, the rat strain F344 has often been used for aging research, although Sprague-Dawley and Wistar rats have also been analyzed. Trabecular bone volume of the vertebra of rats reportedly does not exhibit a decrease at 12 months of age, in contrast to mice[31,32,34,35]; however, although the time course and structural changes in bone aging phenotypes differ between these rodents, both experience age-related bone loss. As a system, mice are advantageous because of the availability of genetic manipulation techniques, but because of their larger size rats represent a more appropriate system to study alterations in the vascular system. It has been suggested that blood vessel aging is associated with senility and the onset of geriatric diseases, and age-related alterations in the skeletal vasculature system also likely promote decreased blood flow in bone. Prosby et al. determined age-related changes in femoral blood flow using rats of 4–6 and 24–26 months of age as models of young adult and aged animals, respectively.[36] Blood flow in aged rats was decreased to 70–80% of levels seen in young controls, and endothelial vasodilation of the principal nutrient artery was significantly reduced in aged animals relative to controls, whereas endothelium-independent vasodilation remained unchanged. The concentration of the intraluminal nitric oxide (NO), a vasodilator, was markedly decreased in the aged artery, suggesting that age-related reduction in NO signaling underlies decreased blood flow. The Louvain (LOU) rat exhibits an increased lifespan and is recognized as a model of healthy aging.[37] Duque et al. reported that aged LOU rats show low-turnover bone metabolism and an increase in bone marrow adiposity, which models the situation seen in human senile osteoporosis (Fig. 10.1).[38] Thus, rats are also useful to evaluate relationships between bone metabolism and physiological, age-related alterations.

10.5 Caloric Restriction

Caloric restriction (CR) is known to extend lifespan in flies, worms, and yeast as well as in mammals.[39,40] CR reduces body mass, which is positively correlated with bone mass. As early as 1935, McCay et al. reported that dietary restriction of laboratory rats increased their lifespan.[41] The authors also found that femoral bone density was decreased by CR, and hypothesized that this might be an indication of growth retardation. Currently, accumulated data indicate that CR delays

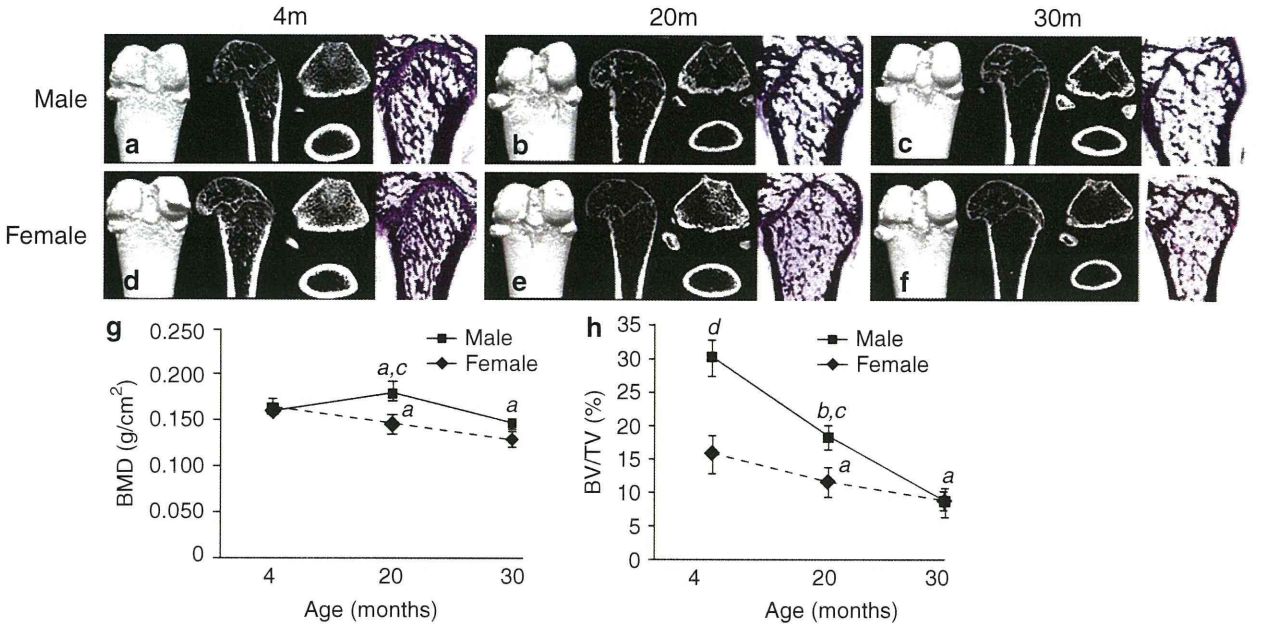

Fig. 10.1 μCT analysis (**a–f**) to evaluate bone structure and sections of undecalcified bone stained with von Kossa (**a–f**, *right panels*) (magnification×10) to evaluate mineralized tissue (*black*) and fat volume (*white*). The figure shows 3D images of the trabecular bone and cross-sectional images of the cortical bone from rats aged 4, 20, and 30 months (**a–f**). The loss in bone volume, the reduction in both trabecular bone and cortical thickness, and the increasing cortical porosity with age are visually apparent. Age-related changes in BMD (**g**) and BV/TV (**h**) showed a significant decline in both groups matching similar levels of bone mass and bone quality at 30 months of age (*Note*: $a - p<0.01$, $b - p<0.001$ compared with 4 months, one-way ANOVA and Dunnett's test; $c - p<0.01$, $d - p<0.001$ males versus females) (From Duque et al.[38])

the progression and/or onset of age-related disorders, such as neurodegeneration, renal failure, cataracts, immune diseases, and cancer malignancy.[42,43] Thus it is plausible that CR could impact age-related bone loss.

Kalu et al. report that male F344 rats undergoing lifelong CR show reduced age-related bone loss via suppression of elevated serum PTH levels.[44] However, Sanderson et al. observed that CR starting at around 17 months of age caused femoral bone loss in Lobund-Wistar rats.[45] In another study, three mouse strains, SENCAR, C57BL/6, and DBA/2, were subjected to a 6-month period of CR, begun at 10 weeks of age.[46] CR increased vertebral BMD in SENCAR and C57BL/6 mice but decreased femoral BMD in SENCAR and DBA/2 mice, indicating that the CR effect is dependent on strain and experimental setting. Ten-week CR, started at 14 weeks of age, reduced serum leptin and IGF-1 levels, and reduced cortical bone thickness, whereas vertebral BMD and trabecular bone volume in mice were significantly increased.[47] Tatsumi et al. reported that the effects of lifelong CR, started at 12 weeks of age, are biphasic on tibial bone metabolism in C57BL/6 mice and F344 rats.[48] By 9 months of CR, trabecular bone mass was decreased compared to control ad libitum fed animals, and bone histomorphometric analyses revealed that the decrease was mainly due to reduced bone formation. However, the difference in bone mass between CR and controls was not significant with longer periods of CR, and bone mass was even higher in CR after 12 months of age, suggesting that CR delays bone aging.[48] Although overall these results differ, CR likely attenuates developmental acquisition of bone volume but delays age-related bone loss.

Recently, it has been reported that administration of rapamycin, an inhibitor of the TOR pathway that acts as nutrient sensor in cells, extends lifespan in yeast, worms, flies, and mice, mimicking CR.[49] The mammalian TOR (mTOR) pathway is known to regulate FOXO signaling, which plays important roles in osteoblast activity.[50,51] The transcription factors FOXO and ATF4 cooperatively regulate expression of osteocalcin, which in an uncarboxylated form acts as a glucose-regulating hormone.[51,52] In addition, FOXO mediates cellular defenses to oxidative stress, and ATF4 regulates expression of *Rankl*.[53,54] Thus, the

mTOR pathway may directly regulate bone metabolism. Future studies should address a potential effect of rapamycin on bone metabolism, especially on age-related bone loss in senile osteoporosis.

10.6 Age-Related Bone Loss

Osteopetrotic animals constitute another classic model of bone disease. Although osteopetrosis represents an opposite phenotype of osteoporosis, age-dependent decreases in bone mass have been reported in osteopetrotic animals. In *op/op* mice, which lack functional M-CSF activity, alleviation of the osteopetrotic phenotype has been observed with age.[55] As noted, both M-CSF and RANKL are essential regulators of osteoclastogenesis, and their expression increases in the bone marrow of aged animals. The alleviation of osteopetrotic phenotypes seen in aging *op/op* mice suggests that an age-dependent factor(s), other than M-CSF and RANKL, plays a role in osteoclastogenesis and may function in age-related acceleration of bone loss, whereas we cannot rule out the possibility that unknown age- or disease-specific factors may compensate for the impairment. Development of DNA microarray techniques has led to expression profiling of various tissues in circumstances including aging. Several studies indicate that upregulation of inflammatory cytokine expression is a common feature of aged tissues and senescent cells.[56-59] Several studies suggest that the activity of nuclear factor κB (NF-κB), a transcriptional regulator of cytokine expression, increases in tissues from animals with age-related disease.[60-62] NF-κB activity, as well as the presence of inflammatory cytokines, is a critical factor in osteoclast formation.[63] Furthermore, tumor necrosis factor (TNF), a well-known inducer of NF-κB activity, is a major adipokine expressed in fat tissues whose mass is significantly reduced in adult CR animals.[64,65] TNF has also been proposed to be a cachexic hormone in various diseases.[66,67] RANKL activity is significantly increased in the presence of TNF.[68,69] Taken together, these observations suggest that age-related upregulation of the NF-κB pathway may function in age-related bone loss, although the pathway has not yet been shown to play a causative role in aging. Thus, a hypothetical aging factor, which stimulates NF-κB pathway or sensitizes cells to NF-κB signaling, may function in age-related bone loss and senile osteoporosis. Age-dependent bone loss is also caused in part by loss of responsiveness to anabolic stimuli, and the hypothetical aging factor(s) may be involved as well. The similar pathophysiology seen between human and animal models suggests that aging factor(s) functioning in senile osteoporosis identified in rodent studies could be shared by humans.

References

1. Ferguson VL, Ayers RA, Bateman TA, Simske SJ. Bone development and age-related bone loss in male C57BL/6J mice. *Bone*. 2003;33(3):387-398.
2. Glatt V, Canalis E, Stadmeyer L, Bouxsein ML. Age-related changes in trabecular architecture differ in female and male C57BL/6J mice. *J Bone Miner Res*. 2007;22(8):1197-1207.
3. Halloran BP, Ferguson VL, Simske SJ, Burghardt A, Venton LL, Majumdar S. Changes in bone structure and mass with advancing age in the male C57BL/6J mouse. *J Bone Miner Res*. 2002;17(6):1044-1050.
4. Hamrick MW, Ding KH, Pennington C, et al. Age-related loss of muscle mass and bone strength in mice is associated with a decline in physical activity and serum leptin. *Bone*. 2006;39(4):845-853.
5. Danilovich N, Sairam MR. Haploinsufficiency of the follicle-stimulating hormone receptor accelerates oocyte loss inducing early reproductive senescence and biological aging in mice. *Biol Reprod*. 2002;67(2):361-369.
6. Hirose S, Li M, Kojima T, et al. A histological assessment on the distribution of the osteocytic lacunar canalicular system using silver staining. *J Bone Miner Metab*. 2007;25(6):374-382.
7. Cao J, Venton L, Sakata T, Halloran BP. Expression of RANKL and OPG correlates with age-related bone loss in male C57BL/6 mice. *J Bone Miner Res*. 2003;18(2):270-277.
8. Cao JJ, Wronski TJ, Iwaniec U, et al. Aging increases stromal/osteoblastic cell-induced osteoclastogenesis and alters the osteoclast precursor pool in the mouse. *J Bone Miner Res*. 2005;20(9):1659-1668.
9. Giustina A, Mazziotti G, Canalis E. Growth hormone, insulin-like growth factors, and the skeleton. *Endocr Rev*. 2008; 29(5):535-559.
10. Linkhart TA, Mohan S, Baylink DJ. Growth factors for bone growth and repair: IGF, TGF beta and BMP. *Bone*. 1996; 19(1 Suppl):1S-12S.
11. Cao JJ, Kurimoto P, Boudignon B, Rosen C, Lima F, Halloran BP. Aging impairs IGF-I receptor activation and induces skeletal resistance to IGF-I. *J Bone Miner Res*. 2007;22(8): 1271-1279.
12. Hodsman AB, Bauer DC, Dempster DW, et al. Parathyroid hormone and teriparatide for the treatment of osteoporosis: a review of the evidence and suggested guidelines for its use. *Endocr Rev*. 2005;26(5):688-703.
13. Knopp E, Troiano N, Bouxsein M, et al. The effect of aging on the skeletal response to intermittent treatment with parathyroid hormone. *Endocrinology*. 2005;146(4):1983-1990.

14. Srinivasan S, Agans SC, King KA, Moy NY, Poliachik SL, Gross TS. Enabling bone formation in the aged skeleton via rest-inserted mechanical loading. *Bone*. 2003;33(6):946-955.
15. Takeda T, Hosokawa M, Takeshita S, et al. A new murine model of accelerated senescence. *Mech Ageing Dev*. 1981; 17(2):183-194.
16. Matsushita M, Tsuboyama T, Kasai R, et al. Age-related changes in bone mass in the senescence-accelerated mouse (SAM). SAM-R/3 and SAM-P/6 as new murine models for senile osteoporosis. *Am J Pathol*. 1986;125(2):276-283.
17. Jilka RL, Weinstein RS, Takahashi K, Parfitt AM, Manolagas SC. Linkage of decreased bone mass with impaired osteoblastogenesis in a murine model of accelerated senescence. *J Clin Invest*. 1996;97(7):1732-1740.
18. Weinstein RS, Jilka RL, Parfitt AM, Manolagas SC. The effects of androgen deficiency on murine bone remodeling and bone mineral density are mediated via cells of the osteoblastic lineage. *Endocrinology*. 1997;138(9):4013-4021.
19. Kodama Y, Takeuchi Y, Suzawa M, et al. Reduced expression of interleukin-11 in bone marrow stromal cells of senescence-accelerated mice (SAMP6): relationship to osteopenia with enhanced adipogenesis. *J Bone Miner Res*. 1998; 13(9):1370-1377.
20. Kajkenova O, Lecka-Czernik B, Gubrij I, et al. Increased adipogenesis and myelopoiesis in the bone marrow of SAMP6, a murine model of defective osteoblastogenesis and low turnover osteopenia. *J Bone Miner Res*. 1997; 12(11):1772-1779.
21. Silva MJ, Brodt MD. Mechanical stimulation of bone formation is normal in the SAMP6 mouse. *Calcif Tissue Int*. 2008;82(6):489-497.
22. Silva MJ, Brodt MD, Ettner SL. Long bones from the senescence accelerated mouse SAMP6 have increased size but reduced whole-bone strength and resistance to fracture. *J Bone Miner Res*. 2002;17(9):1597-1603.
23. Silva MJ, Brodt MD, Ko M, Abu-Amer Y. Impaired marrow osteogenesis is associated with reduced endocortical bone formation but does not impair periosteal bone formation in long bones of SAMP6 mice. *J Bone Miner Res*. 2005; 20(3):419-427.
24. Ichioka N, Inaba M, Kushida T, et al. Prevention of senile osteoporosis in SAMP6 mice by intrabone marrow injection of allogeneic bone marrow cells. *Stem Cells*. 2002;20(6): 542-551.
25. Takada K, Inaba M, Ichioka N, et al. Treatment of senile osteoporosis in SAMP6 mice by intra-bone marrow injection of allogeneic bone marrow cells. *Stem Cells*. 2006; 24(2):399-405.
26. Ueda Y, Inaba M, Takada K, et al. Induction of senile osteoporosis in normal mice by intra-bone marrow-bone marrow transplantation from osteoporosis-prone mice. *Stem Cells*. 2007;25(6):1356-1363.
27. Nakanishi R, Shimizu M, Mori M, et al. Secreted frizzled-related protein 4 is a negative regulator of peak BMD in SAMP6 mice. *J Bone Miner Res*. 2006;21(11):1713-1721.
28. Shimizu M, Higuchi K, Kasai S, et al. Chromosome 13 locus, Pbd2, regulates bone density in mice. *J Bone Miner Res*. 2001;16(11):1972-1982.
29. Shimizu M, Higuchi K, Bennett B, et al. Identification of peak bone mass QTL in a spontaneously osteoporotic mouse strain. *Mamm Genome*. 1999;10(2):81-87.
30. Banu J, Wang L, Kalu DN. Age-related changes in bone mineral content and density in intact male F344 rats. *Bone*. 2002;30(1):125-130.
31. Kiebzak GM, Smith R, Gundberg CC, Howe JC, Sacktor B. Bone status of senescent male rats: chemical, morphometric, and mechanical analysis. *J Bone Miner Res*. 1988;3(1): 37-45.
32. Kiebzak GM, Smith R, Howe JC, Gundberg CM, Sacktor B. Bone status of senescent female rats: chemical, morphometric, and biomechanical analyses. *J Bone Miner Res*. 1988; 3(4):439-446.
33. Turner CH, Takano Y, Owan I. Aging changes mechanical loading thresholds for bone formation in rats. *J Bone Miner Res*. 1995;10(10):1544-1549.
34. Wang L, Banu J, McMahan CA, Kalu DN. Male rodent model of age-related bone loss in men. *Bone*. 2001;29(2): 141-148.
35. Barbier A, Martel C, de Vernejoul MC, et al. The visualization and evaluation of bone architecture in the rat using three-dimensional X-ray microcomputed tomography. *J Bone Miner Metab*. 1999;17(1):37-44.
36. Prisby RD, Ramsey MW, Behnke BJ, et al. Aging reduces skeletal blood flow, endothelium-dependent vasodilation, and NO bioavailability in rats. *J Bone Miner Res*. 2007; 22(8):1280-1288.
37. Alliot J, Boghossian S, Jourdan D, et al. The LOU/c/jall rat as an animal model of healthy aging? *J Gerontol A Biol Sci Med Sci*. 2002;57(8):B312-B320.
38. Duque G, Rivas D, Li W, et al. Age-related bone loss in the LOU/c rat model of healthy ageing. *Exp Gerontol*. 2009; 44(3):183-189.
39. Mair W, Dillin A. Aging and survival: the genetics of life span extension by dietary restriction. *Annu Rev Biochem*. 2008;77:727-754.
40. Sohal RS, Weindruch R. Oxidative stress, caloric restriction, and aging. *Science*. 1996;273(5271):59-63.
41. McCay CM, Crowell MF, Maynard LA. The effect of retarded growth upon the length of life span and upon the ultimate body size. *J Nutr*. 1935;10:63-79.
42. Masoro EJ. Overview of caloric restriction and ageing. *Mech Ageing Dev*. 2005;126(9):913-922.
43. Weindruch R, Sohal RS. Seminars in medicine of the Beth Israel Deaconess Medical Center. Caloric intake and aging. *N Engl J Med*. 1997;337(14):986-994.
44. Kalu DN, Hardin RH, Cockerham R, Yu BP. Aging and dietary modulation of rat skeleton and parathyroid hormone. *Endocrinology*. 1984;115(4):1239-1247.
45. Sanderson JP, Binkley N, Roecker EB, et al. Influence of fat intake and caloric restriction on bone in aging male rats. *J Gerontol A Biol Sci Med Sci*. 1997;52(1):B20-B25.
46. Brochmann EJ, Duarte ME, Zaidi HA, Murray SS. Effects of dietary restriction on total body, femoral, and vertebral bone in SENCAR, C57BL/6, and DBA/2 mice. *Metabolism*. 2003;52(10):1265-1273.
47. Hamrick MW, Ding KH, Ponnala S, Ferrari SL, Isales CM. Caloric restriction decreases cortical bone mass but spares trabecular bone in the mouse skeleton: implications for the regulation of bone mass by body weight. *J Bone Miner Res*. 2008;23(6):870-878.
48. Tatsumi S, Ito M, Asaba Y, Tsutsumi K, Ikeda K. Life-long caloric restriction reveals biphasic and dimorphic effects on

bone metabolism in rodents. *Endocrinology*. 2008;149(2): 634-641.
49. Katewa SD, Kapahi P. Dietary restriction and aging, 2009. *Aging Cell*. 2010;9(2):105-112.
50. Ambrogini E, Almeida M, Martin-Millan M, et al. FoxO-mediated defense against oxidative stress in osteoblasts is indispensable for skeletal homeostasis in mice. *Cell Metab*. 2010;11(2):136-146.
51. Rached MT, Kode A, Xu L, et al. FoxO1 is a positive regulator of bone formation by favoring protein synthesis and resistance to oxidative stress in osteoblasts. *Cell Metab*. 2010;11(2):147-160.
52. Rached MT, Kode A, Silva BC, et al. FoxO1 expression in osteoblasts regulates glucose homeostasis through regulation of osteocalcin in mice. *J Clin Invest*. 2010;120(1): 357-368.
53. Elefteriou F, Ahn JD, Takeda S, et al. Leptin regulation of bone resorption by the sympathetic nervous system and CART. *Nature*. 2005;434(7032):514-520.
54. Manolagas SC, Almeida M. Gone with the Wnts: beta-catenin, T-cell factor, forkhead box O, and oxidative stress in age-dependent diseases of bone, lipid, and glucose metabolism. *Mol Endocrinol*. 2007;21(11):2605-2614.
55. Begg SK, Bertoncello I. The hematopoietic deficiencies in osteopetrotic (op/op) mice are not permanent, but progressively correct with age. *Exp Hematol*. 1993;21(4):493-495.
56. Blalock EM, Chen KC, Sharrow K, et al. Gene microarrays in hippocampal aging: statistical profiling identifies novel processes correlated with cognitive impairment. *J Neurosci*. 2003;23(9):3807-3819.
57. Lee CK, Klopp RG, Weindruch R, Prolla TA. Gene expression profile of aging and its retardation by caloric restriction. *Science*. 1999;285(5432):1390-1393.
58. Melov S, Hubbard A. Microarrays as a tool to investigate the biology of aging: a retrospective and a look to the future. *Sci Aging Knowl Environ*. 2004;2004(42):re7.
59. Coppe JP, Desprez PY, Krtolica A, Campisi J. The senescence-associated secretory phenotype: the dark side of tumor suppression. *Annu Rev Pathol*. 2010;5:99-118.
60. Gosselin K, Abbadie C. Involvement of Rel/NF-kappa B transcription factors in senescence. *Exp Gerontol*. 2003; 38(11–12):1271-1283.
61. Pasparakis M. Regulation of tissue homeostasis by NF-kappaB signalling: implications for inflammatory diseases. *Nat Rev Immunol*. 2009;9(11):778-788.
62. Sarkar D, Fisher PB. Molecular mechanisms of aging-associated inflammation. *Cancer Lett*. 2006;236(1):13-23.
63. Novack DV, Teitelbaum SL. The osteoclast: friend or foe? *Annu Rev Pathol*. 2008;3:457-484.
64. Hwang CS, Loftus TM, Mandrup S, Lane MD. Adipocyte differentiation and leptin expression. *Annu Rev Cell Dev Biol*. 1997;13:231-259.
65. Moller DE, Kaufman KD. Metabolic syndrome: a clinical and molecular perspective. *Annu Rev Med*. 2005;56:45-62.
66. Spiegelman BM, Hotamisligil GS. Through thick and thin: wasting, obesity, and TNF alpha. *Cell*. 1993;73(4):625-627.
67. Tracey KJ, Cerami A. Tumor necrosis factor: a pleiotropic cytokine and therapeutic target. *Annu Rev Med*. 1994;45:-491-503.
68. Chambers TJ. Regulation of the differentiation and function of osteoclasts. *J Pathol*. 2000;192(1):4-13.
69. Xing L, Schwarz EM, Boyce BF. Osteoclast precursors, RANKL/RANK, and immunology. *Immunol Rev*. 2005; 208:19-29.